PHYSICAL REVIEW D **84,** 123501 (2011)

Notes on ghost dark energy

Rong-Gen Cai,* Zhong-Liang Tuo,† and Hong-Bo Zhang‡
Key Laboratory of Frontiers in Theoretical Physics, Institute of Theoretical Physics, Chinese Academy of Sciences, P.O. Box 2735, Beijing 100190, China

Qiping Su§
Department of Physics, Hangzhou Normal University, Hangzhou, 310036, China
(Received 7 September 2011; published 2 December 2011)

We study a phenomenological dark energy model which is rooted in the Veneziano ghost of QCD. In this dark energy model, the energy density of dark energy is proportional to Hubble parameter and the proportional coefficient is of the order $\Lambda_{\rm QCD}^3$, where $\Lambda_{\rm QCD}$ is the mass scale of QCD. The universe has a de Sitter phase at late time and begins to accelerate at redshift around $z_{\rm acc} \sim 0.6$. We fit this model and give the constraints on model parameters, with current observational data including Type Ia supernovea, baryon acoustic oscillation, cosmic microwave background, big bang nucleosynthesis, and Hubble parameter data. We also study the cosmological evolution of the dark energy with interaction with cold dark matter.

DOI: 10.1103/PhysRevD.84.123501 PACS numbers: 98.80.−k, 12.38.−t, 95.35.+d, 95.36.+x

I. INTRODUCTION

It has been more than ten years since our universe was found to be in accelerating expansion [1]. A new energy component of the universe, called dark energy (DE), is needed to explain this acceleration. The simplest model of DE is the cosmological constant, which is a key ingredient in the ΛCDM model. Although the ΛCDM model is consistent very well with all observational data, it faces with the fine tuning problem [2]. Plenty of other DE models have also been proposed [3–9], but almost all of them explain the acceleration expansion either by introducing new degree(s) of freedom or by modifying gravity.

Recently a new DE model, so-called Veneziano ghost DE, has been proposed [10,11]. The key ingredient of this new model is that the Veneziano ghost, which is unphysical in the usual Minkowski spacetime Quantum Field Theory, exhibits important physical effects in dynamical spacetime or spacetime with nontrivial topology. Veneziano ghost is supposed to exist for solving the $U(1)$ problem in low-energy effective theory of QCD [12–16]. The ghost has no contribution to the vacuum energy density in Minkowski spacetime, but, in a curved spacetime, it gives rise to a small vacuum energy density proportional to $\Lambda_{\rm QCD}^3 H$ [17–20], where $\Lambda_{\rm QCD}$ is QCD mass scale and H is Hubble parameter. Note that in this ghost dark energy model, there are no unwanted features such as violation of gauge invariance, unitarity, causality, etc. [10,11,17–20]. In fact, the description in terms of the Veneziano ghost is just a matter of convenience to describe very complicated infrared dynamics of strongly coupled QCD as the Veneziano ghost is not a physical propagating degree of freedom. One can describe the same dynamics using some other approaches (e.g. direct lattice simulations) without using the ghost. Therefore the Veneziano ghost field is quite different from those ghost fields in some dark energy models in the literature, there those ghost fields are real physical degrees of freedom, introduced in order to have the equation of state of dark energy to cross -1. On the other hand, the vacuum energy is generally expected exponentially suppressed because QCD is a theory with a mass gap, rather than is linear in Hubble parameter. This issue is elaborated in some details in [17–20], there it has been convincingly argued that the complicated topological structure of strongly coupled QCD may lead to the linear correction.

Because this model is totally embedded in standard model and general relativity, one needs not to introduce any new parameter, new degree of freedom, or to modify gravity. With $\Lambda_{\rm QCD} \sim 100$ MeV and $H \sim 10^{-33}$ eV, $\Lambda_{\rm QCD}^3 H$ gives the right order of observed DE energy density. This numerical coincidence is impressive and also means that this model gets rid of the fine tuning problem [10,11]. Actually, several authors have already suggested DE model with energy density proportional to $\Lambda_{\rm QCD}^3 H$ in different physical contexts [21–27] such as QCD trace anomaly, gluon condensate of quantum chromodynamics, modifying gravity, and so on.

In this work, we investigate the phenomenological model with energy density $\rho_{\rm DE}$ proportional to Hubble parameter H. We study the cosmological evolution of the DE model with/without interaction between the DE and dark matter. We analytically and numerically compute some quantities such as scale factor a, $\rho_{\rm DE}$, squared adiabatic speed of sound c_s^2, and so on. Also we fit this model

*cairg@itp.ac.cn
†tuozhl@itp.ac.cn
‡hbzhang@itp.ac.cn
§sqp@itp.ac.cn

with current observational data and give constraints on the model parameters.

This note is organized as follows. In Sec. II we study the dynamical evolution of the DE model. In Sec. III, we fit this model with current observational data and discuss the fitting results. The data used are Union II SnIa sample [28], BAO data from SDSS DR7 [29], CMB data (R, l_a, z_*) from WMAP7 [30], 12 Hubble evolution data [31,32], and big bang nucleosynthesis (BBN) [33,34]. In Sec. IV, we introduce the interaction between DE and cold dark matter (CDM) and study the dynamical evolution in this case. We summary our work and give some discussions in Sec. V.

II. DYNAMICS OF GHOST DARK ENERGY

To study the dynamics of the DE model, we consider a flat Friedmann-Robertson-Walker (FRW) universe with only two energy components, CDM and DE, and neglect radiation and baryon temporarily in this section. We will include the radiation and baryon when fit the model with observational data in Sec. IV.

In this ghost DE model, the energy density of DE is given by $\rho_{\rm DE} = \alpha H$, where α is a constant with dimension [energy]^3 and roughly of order of $\Lambda^3_{\rm QCD}$, where $\Lambda_{\rm QCD} \sim 100$ MeV is QCD mass scale. Arming with this DE density, the Friedman equation reads

$$H^2 = \frac{8\pi G}{3}(\alpha H + \rho_m), \tag{1}$$

where ρ_m is energy density of CDM, whose continuity equation gives

$$\dot{\rho}_m + 3H\rho_m = 0 \Rightarrow \rho_m = \rho_{m0}a^{-3}. \tag{2}$$

We have set $a_0 = 1$ and the subscript 0 stands for the present value of some quantity. From (1) and (2), we can obtain the Raychaudhuri equation

$$\dot{H} + H^2 = -\frac{4\pi G}{3}\left[-\rho_{\rm DE}\left(\frac{\dot{\rho}_{\rm DE}}{H\rho_{\rm DE}} + 2\right) + \rho_m\right]. \tag{3}$$

Solving the Friedman equation, we have

$$H_\pm = \frac{4\pi G}{3}\alpha \pm \sqrt{\left(\frac{4\pi G}{3}\alpha\right)^2 + \frac{8\pi G}{3}\rho_{m0}a^{-3}}. \tag{4}$$

There are two branches, H_+ represents an expansion solution, while H_- a contraction one. We neglect the latter since it goes against the observation and, for simplicity, write H_+ as H in what follows.

Before preceding, let us notice that (1) is exactly the same as that in Dvali-Gabadadze-Porrati (DGP) model [35] with crossover scale $r_c = 1/\alpha$ in Planck unit. However, this ghost DE model is essentially different from DGP model. At first, although the Friedmann equation is the same for both models for a flat FRW universe, in a *nonflat* universe with spatial curvature κ ($\kappa \neq 0$), the Friedman equation in the ghost DE model reads

$$H^2 + \frac{\kappa}{a^2} = \frac{8\pi G}{3}(\rho + \alpha H), \tag{5}$$

while in the DGP model, the Friedman equation is

$$H^2 + \frac{\kappa}{a^2} - \frac{1}{r_c}\sqrt{H^2 + \frac{\kappa}{a^2}} = \frac{8\pi G}{3}\rho. \tag{6}$$

They are clearly different. Second, the DGP model is essentially a five dimensional one, and it is a brane-world scenario (for a review on brane-world gravity see [36]), while the ghost DE model is a four dimensional one, and it is in the realm of general relativity. Therefore even for a flat universe, they are different at the linear perturbation level. As a result, it is of some interest to further study the perturbation theory of the ghost DE model, which is currently under investigation.

Now we continue our discussion of the ghost DE model, we define a characteristic scale factor a_*

$$a_* \equiv \left(\frac{12\rho_{m0}}{8\pi G\alpha^2}\right)^{1/3} = \left(4\frac{\Omega_{m0}}{\Omega^2_{\rm DE0}}\right)^{1/3} = 10^2\left(36\Omega_{m0}\frac{\rm MeV^6}{\alpha^2}\right)^{1/3},$$

where we have taken $H_0 = 10^{-33}$ eV, Ω_{m0} and $\Omega_{\rm DE0}$ are the dimensionless energy density of CDM and DE, respectively. One can see shortly that actually a_* is the transition point when the universe transits from the dust phase to a de Sitter phase. If we assume $\Omega_{m0} = \frac{1}{4}$ and $\Omega_{\rm DE0} = \frac{3}{4}$, by definition, we get roughly $a_* \sim 1$, which means that the transition occurs just at present. Therefore, we will take $a_* = 1$ throughout this section. And especially $\alpha \sim$ (10 MeV)^3 if $a_* \sim 1$.

At early epoch $a \ll a_* \sim 1$, the a^{-3} term dominates in (4), the Hubble parameter behaves like $H \sim a^{-(3/2)}$, which means that the universe is in a dust phase. While at late epoch $a \gg a_* \sim 1$, the a^0 term dominates in (4), as a result, $H =$ const, which says that the universe enters a de Sitter phase at late time. Here a_* is the transition point between these two phases as mentioned above.

We can solve (4) analytically as

$$4\pi G\alpha(t - t_i) = -x^3 + x^3\sqrt{1 + x^{-3}} + \frac{3}{2}\ln x + \ln\left(1 + \sqrt{1 + x^{-3}}\right),$$

where $x = \frac{a}{a_*}$ and t_i is the initial time when $a(t_i) = 0$. At early time $x \ll 1$, $4\pi G\alpha(t - t_i) = 2x^{3/2}$; while at late time $x \gg 1$, $4\pi G\alpha(t - t_i) = \frac{3}{2}\ln x$. These asymptotic behaviors agree with the previous argument. The numerical relation $t \sim a$ is plotted in Fig. 1.

Using (4) and the definition of $\rho_{\rm DE}$, we have the energy density of DE as

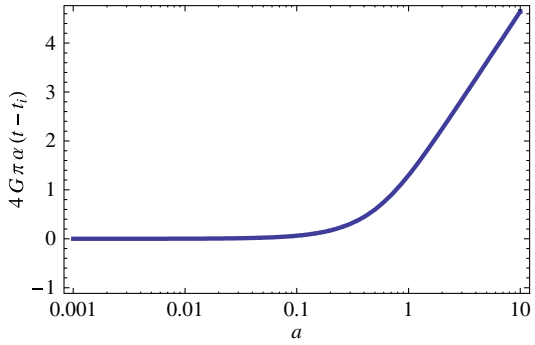

FIG. 1 (color online). $4\pi G\alpha(t - t_i) \sim a$, where $a_* = 1$.

$$\rho_{\rm DE} = \alpha H = \frac{4\pi G}{3}\alpha^2\left[1 + \sqrt{1 + \left(\frac{a_*}{a}\right)^3}\right].$$

The behavior of $\rho_{\rm DE}$ in terms of a is shown in Fig. 2. The equation of state (EoS) of the ghost DE is given by

$$\begin{aligned}\omega &\equiv -\frac{1}{3}\frac{\dot\rho_{\rm DE}}{H\rho_{\rm DE}} - 1 \\ &= \frac{1}{2}\left(\frac{a_*}{a}\right)^3\left(\frac{1}{\sqrt{1 + (\frac{a_*}{a})^3}} - \frac{1}{1 + \sqrt{1 + (\frac{a_*}{a})^3}}\right) - 1 \\ &= \begin{cases} -\frac{1}{2} & a \ll a_* \\ -1 & a \gg a_* \end{cases}. \end{aligned} \tag{7}$$

From the asymptotic behavior of ω, we can see that the DE acts like a cosmological constant at late time. We plot the relation $\omega \sim a$ in Fig. 3. From the figure, we can see that ω can never cross -1, which is similar to the behavior of quintessence. We will show that this behavior can be altered in the presence of interaction between DE and CDM in Sec. IV. ω varies from $-\frac{1}{2}$ at early time to -1 at late time, which is similar to freezing quintessence model [37]. We can also find that ω has a sharp variation round $a = a_*$. It is easy to understand if we rewrite the expression of ω as

$$3(1 + \omega) = -\frac{\dot\rho_{\rm DE}}{H\rho_{\rm DE}} = -\frac{\dot H}{H^2} = (H^{-1})^{\cdot}, \tag{8}$$

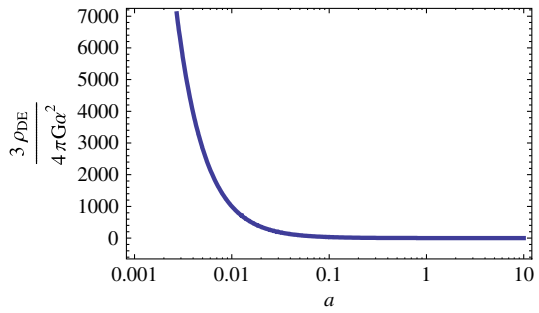

FIG. 2 (color online). $\frac{3H}{4\pi G\alpha} \sim a$, where $a_* = 1$.

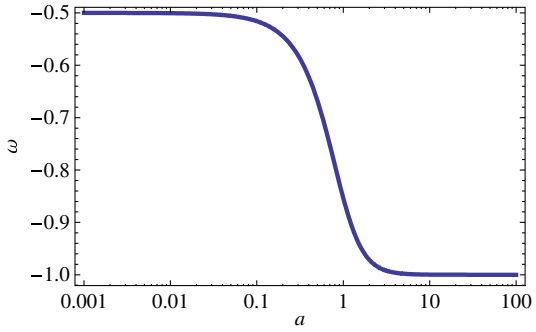

FIG. 3 (color online). $\omega \sim a$, where $a_* = 1$.

from this equation, we can see that in this model the EOS of DE tightly relates to the variation of Hubble parameter, which is quite different in different phases of the universe. For instance, in the dust phase, $(H^{-1})^{\cdot} \sim \frac{3}{2}$, while in the de Sitter phase, $(H^{-1})^{\cdot} \sim 0$. Therefore, there will be a jump from $-\frac{1}{2}$ to -1 when the universe transits from the dust phase to the de Sitter phase.

One can easily show that the EoS of the ghost DE model is $\omega = -\frac{1}{\Omega_m + 1}$. The value ω_0 at present is

$$\omega_0(a = 1) = \frac{1}{\Omega_{\rm DE0} - 2} = -\frac{1}{\Omega_{m0} + 1}, \tag{9}$$

where we have used $a_* = (4\frac{\Omega_{m0}}{\Omega_{\rm DE0}^2})^{1/3}$ in the first equality. This relation is important and helpful to understand the fitting results in Sec. III.

Also from Raychaudhuri Eq. (3), we can get the total equation of state of the universe

$$\omega_{\rm tot} = -1 - \frac{2}{3}\frac{\dot H}{H^2} = 1 + 2\omega = \begin{cases} 0 & a \ll a_* \\ -1 & a \gg a_*. \end{cases} \tag{10}$$

$\omega_{\rm tot}$ decreases monotonically from 0 to -1, which means that the expansion of the universe switches from deceleration at early epoch to acceleration at late epoch. The conversion occurs at $a_{\rm acc}$ when $\omega_{\rm tot}(a_{\rm acc}) = -\frac{1}{3}$. From (7) and (10), we can calculate $a_{\rm acc} = \frac{a_*}{2} \sim 0.5$, which means that the universe begin to accelerate at redshift $z_{\rm acc} \sim 1$.

It is also interesting to study the adiabatic speed of sound. The squared adiabatic sound speed of the ghost DE model is found to be

$$c_s^2 = \frac{\dot p}{\dot\rho_{\rm DE}} = -\frac{1}{2}\frac{1}{(\frac{a}{a_*})^3 + 1} < 0,$$

where the pressure $p = \omega\rho$. The evolution behavior of the squared adiabatic sound speed is shown in Fig. 4. One can see from the figure that c_s^2 leaps from $-\frac{1}{2}$ to 0 at the time a_*. Before a_*, c_s^2 is less than zero, but after $a_* \sim 1$, c_s^2 approximates to zero. Notice that it is always negative Note that the negative speed of sound should not be treated as a signal for instability of this dark energy model since

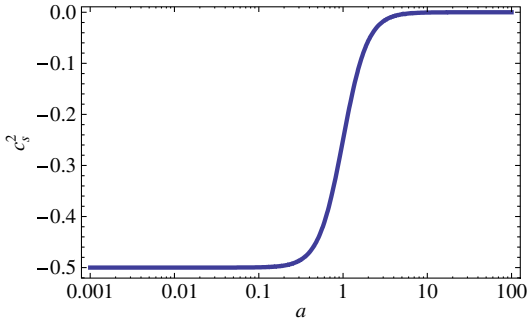

FIG. 4 (color online). $c_s^2 \sim a$, where $a_* = 1$.

the Veneziano ghost is not a propagating physical degree of freedom as mentioned above. A notion of the speed of sound does not exist for a nonphysical, nonpropagating degree of freedom. Such an ''apparent signal for instability'' is in fact a result of treatment of the Veneziano ghost as the conventional physical degree of freedom satisfying classical equation of motion.

In addition, let us stress here that even a physical negative squared adiabatic sound speed will not certainly lead to a potential instability since the stability of a system is determined by the so-called dynamical sound speed instead of the adiabatic sound speed. Dynamical sound speed and adiabatic sound speed may be the same in some cases, but they are different in general. For example, in the case of a slowly rolling scalar field, the squared adiabatic sound speed is -1, while the squared dynamical sound speed is 1. For a discussion for the difference between these two sound speeds, see [38], for example. Such a situation also appears in the so-called kinetic gravity braiding [39].

III. DATA FITTING

A. Model

In order to fit the model with current observational data, we consider a more realistic model which includes DE, CDM, radiation, and baryon in a flat FRW universe in this section. In this case, the Friedman equation reads

$$H^2 = \frac{8\pi G}{3}(\alpha H + \rho_{\rm DM} + \rho_b + \rho_r),$$

which can be rewritten as

$$E \equiv \frac{H}{H_0} = \frac{1}{2}\Omega_{\rm DE0} + \sqrt{\frac{1}{4}\Omega_{\rm DE0}^2 + (\Omega_{\rm DM0} + \Omega_{b0})(1+z)^3 + \Omega_{r0}(1+z)^4},$$

where $\Omega_{\rm DM0}$, Ω_{b0}, Ω_{r0} are present values of dimensionless energy density for CDM, baryon, and radiation, respectively. $\Omega_{\rm DE0} = \frac{8\pi G\alpha}{3H_0}$ is dimensionless energy density of DE at present. Energy density of baryon and CDM are always written together as $\Omega_{\rm DM0} + \Omega_{b0} = \Omega_{m0}$. Notice that $\Omega_{\rm DE0} + \Omega_{m0} + \Omega_{r0} = 1$ since we assume a flat universe. The energy density of radiation is the sum of those of photons and relativistic neutrinos

$$\Omega_{r0} = \Omega_{\gamma 0}(1 + 0.2271 N_n),$$

where $N_n = 3.04$ is the effective number of neutrino species, and $\Omega_{\gamma 0} = 2.469 \times 10^{-5} h^{-2}$ for $T_{\rm cmb} = 2.725K$ ($h = H_0/100$ Mpc $\cdot$ km $\cdot$ s^{-1}).

It is worth noticing that from the definition of dimensionless energy density of DE and flatness of our universe we can get an important relation [see also (19)]

$$(1 - \Omega_{m0})H_0 = \frac{8\pi G\alpha}{3} = \text{const}, \tag{11}$$

where we have neglected Ω_{r0}, which is very small compared to Ω_{m0}. It means that parameters Ω_{m0}, h, and α are closely related; α can be expressed in terms of Ω_{m0} and h. We will choose Ω_{m0}, h, and Ω_{b0} as free parameters of the model in the following analysis. This relation also infers that there exists a strong degeneracy between Ω_{m0} and h, as shown in Sec. III C.

B. Sets of observational data

We fit our model by employing some observational data including SnIa, BAO, CMB, Hubble evolution data, and BBN.

The data for SnIa are the 557 Uion II sample [28]. $\chi^2_{\rm sn}$ for SnIa is obtained by comparing theoretical distance modulus $\mu_{\rm th}(z) = 5\log_{10}[(1+z)\int_0^z dx/E(x)] + \mu_0$ ($\mu_0 = 42.384 - 5\log_{10}h$) with observed $\mu_{\rm ob}$ of supernovae:

$$\chi^2_{\rm sn} = \sum_i^{557} \frac{[\mu_{\rm th}(z_i) - \mu_{\rm ob}(z_i)]^2}{\sigma^2(z_i)}.$$

To reduce the effect of μ_0, we expand $\chi^2_{\rm sn}$ with respect to μ_0 [40]:

$$\chi^2_{\rm sn} = A + 2B\mu_0 + C\mu_0^2, \tag{12}$$

where

$$A = \sum_i \frac{[\mu_{\rm th}(z_i;\mu_0 = 0) - \mu_{\rm ob}(z_i)]^2}{\sigma^2(z_i)},$$

$$B = \sum_i \frac{\mu_{\rm th}(z_i;\mu_0 = 0) - \mu_{\rm ob}(z_i)}{\sigma^2(z_i)},$$

$$C = \sum_i \frac{1}{\sigma^2(z_i)}$$

(12) has a minimum as

$$\tilde{\chi}^2_{\rm sn} = \chi^2_{\rm sn,min} = A - B^2/C,$$

which is independent of μ_0. In fact, it is equivalent to performing an uniform marginalization over μ_0; the

TABLE I. The best-fit values with 1σ and 2σ errors for Ω_{m0}, h, and Ω_{b0} in the ghost dark energy model.

Parameter	Ω_{m0}	h	Ω_{b0}
Best-fit$^{-1\sigma,-2\sigma}_{+1\sigma,+2\sigma}$	$0.257^{-0.016,-0.026}_{+0.009,+0.020}$	$0.662^{-0.011,-0.019}_{+0.011,+0.021}$	$0.054^{-0.002,-0.004}_{+0.001,+0.002}$

difference between $\tilde{\chi}^2_{\rm sn}$ and the marginalized $\chi^2_{\rm sn}$ is just a constant [40]. We will adopt $\tilde{\chi}^2_{\rm sn}$ as the goodness of fit between theoretical model and SnIa data.

The second set of data is the Baryon Acoustic Oscillations (BAO) data from Sloan Digital Sky Survey Data Release 7 (SDSS DR7) [29], the datapoints we use are

$$d_{0.2} = \frac{r_s(z_d)}{D_V(0.2)}$$

and

$$d_{0.35} = \frac{r_s(z_d)}{D_V(0.35)},$$

where $r_s(z_d)$ is the comoving sound horizon at the baryon drag epoch [41], and

$$D_V(z) = \left[\left(\int_0^z \frac{dx}{H(x)}\right)^2 \frac{z}{H(z)}\right]^{1/3}$$

encodes the visual distortion of a spherical object due to the non Euclidianity of a FRW spacetime. The inverse covariance matrix of BAO is

$$C^{-1}_{M,\rm bao} = \begin{pmatrix} 30124 & -17227 \\ -17227 & 86977 \end{pmatrix}.$$

The χ^2 of the BAO data is constructed as

$$\chi^2_{\rm bao} = Y^T C^{-1}_{M,\rm bao} Y,$$

where

$$Y = \begin{pmatrix} d_{0.2} - 0.1905 \\ d_{0.35} - 0.1097 \end{pmatrix}.$$

The CMB data points we will use are (R, l_a, z_*) from WMAP7 [30]. z_* is the redshift of recombination [42], R is the scaled distance to recombination

$$R = \sqrt{\Omega^{(0)}_m} \int_0^{z_*} \frac{dz}{E(z)},$$

and l_a is the angular scale of the sound horizon at recombination

$$l_a = \pi \frac{r(a_*)}{r_s(a_*)},$$

where $r(z) = \int_0^z dx/H(x)$ is the comoving distance, and $r_s(a_*)$ is the comoving sound horizon at recombination

$$r_s(a_*) = \int_0^{a_*} \frac{c_s(a)}{a^2 H(a)} da,$$

where the sound speed $c_s(a) = 1/\sqrt{3(1+\bar{R}_b a)}$, and $\bar{R}_b = 3\Omega^{(0)}_b/4\Omega^{(0)}_\gamma$ is the photon-baryon energy density ratio.

The χ^2 of the CMB data is constructed as:

$$\chi^2_{\rm cmb} = X^T C^{-1}_{M,\rm cmb} X,$$

where

$$X = \begin{pmatrix} l_a - 302.09 \\ R - 1.725 \\ z_* - 1091.3 \end{pmatrix},$$

and the inverse covariance matrix

$$C^{-1}_{M,\rm cmb} = \begin{pmatrix} 2.305 & 29.698 & -1.333 \\ 29.698 & 6825.270 & -113.180 \\ -1.333 & -113.180 & 3.414 \end{pmatrix}.$$

The fourth set of observational data is 12 Hubble evolution data from [31,32]. Its χ^2_H is defined as

$$\chi^2_H = \sum_{i=1}^{12} \frac{[H(z_i) - H_{\rm ob}(z_i)]^2}{\sigma_i^2}.$$

Note that the redshift of these data falls in the region $z \in (0, 1.75)$.

The last set we will use is the BBN data from [33,34], whose χ^2 is

$$\chi^2_{\rm bbn} = \frac{(\Omega_{b0}h^2 - 0.022)^2}{0.002^2}.$$

In summary, we have

$$\chi^2_{\rm tot} = \tilde{\chi}^2_{\rm sn} + \chi^2_{\rm cmb} + \chi^2_{\rm bao} + \chi^2_H + \chi^2_{bbn},$$

and we assume uniform priors on all the parameters.

C. Fitting results

The best-fit values and errors of parameters are summarized in Table I. We also list the best-fit values of the corresponding parameters for ΛCDM model in Table II for comparison. The best-fit values of Ω_{m0} and h are slightly smaller than corresponding ones in the ΛCDM

TABLE II. The best-fit values for the ΛCDM model, using the same data sets.

Parameter	Ω_{m0}	h	Ω_{b0}
Best-fit	0.273	0.703	0.045

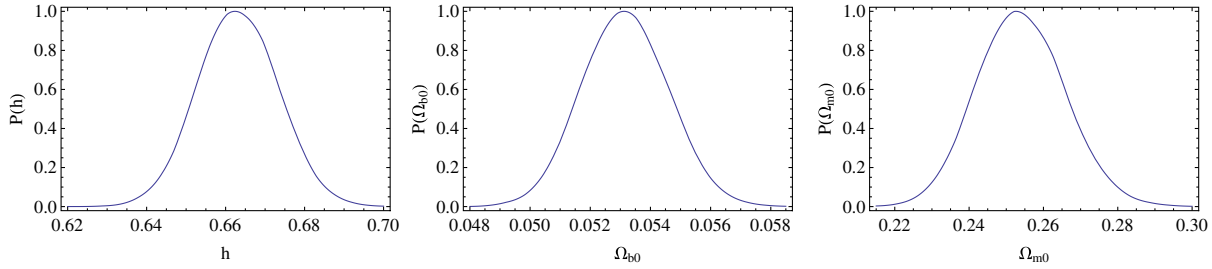

FIG. 5 (color online). One dimensional marginalized distribution probability of h, Ω_{b0}, and Ω_{m0}.

model. In Fig. 5, we plot the one-dimensional marginalized distribution probability of each parameter. The two-dimensional contour is plotted in Fig. 6, from which we can see that there exists a strong correlation between Ω_{m0} and h as we expected in Sec. III A.

With the best-fit value of $\Omega_{m0} = 0.257$, the transition between the dust phase and the de Sitter phase occurs at $a_* = (4\frac{\Omega_{m0}}{\Omega_{\rm DE}^2})^{1/3} = 1.23$. The universe begins to accelerate at $a_{\rm acc} = \frac{a_*}{2} = 0.615$, or in terms of redshift, $z_{\rm acc} = 0.625$. And the present EoS of DE $\omega_0 = -\frac{1}{\Omega_{m0}+1} = -0.796$.

χ^2 of best-fit value of this model is $\chi^2_{\rm min} = 607.192$ for dof $= 575$. The reduced χ^2 equals to 1.056 which is acceptable. But $\chi^2_{\rm min}$ is larger than the one for the ΛCDM model, $\chi^2_{\Lambda\rm CDM} = 554.264$. A similar conclusion is also reached by other authors using different data set [43].

It is not hard to understand why in this model, $\chi^2_{\rm min}$, is large compared to the ΛCDM model. Recently many model independent studies on dynamics of DE show that current observational data favor $\omega \sim -1$, at least at low redshift [44]. But from (9) we can see that $\omega_0 \sim -1$ requires a small Ω_{m0} ($\Omega_{m0} \sim 0$), which goes against CMB and BAO observation. As a result, when we combine these different observational data sets to do joint likelihood analysis, the final χ^2 becomes large.

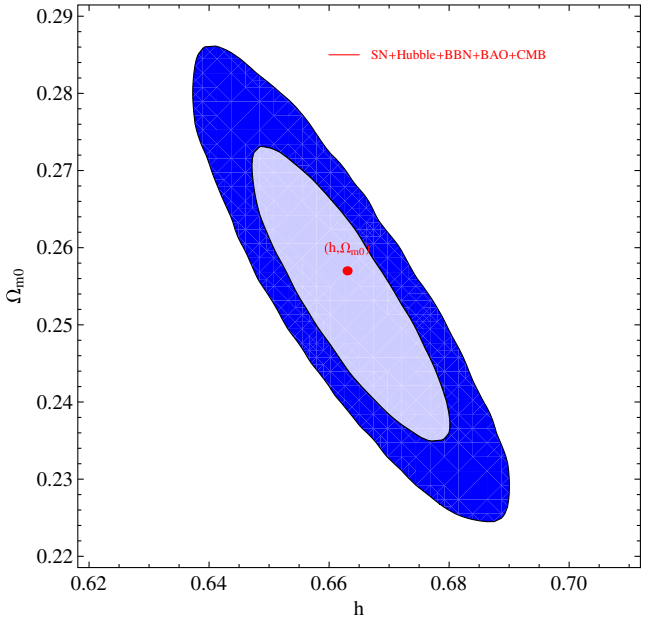

FIG. 6 (color online). 68% and 95% contour plot in $\Omega_{m0} - h$ plane. The red dot in the figure stands for the best-fit value.

IV. INTERACTION BETWEEN DE AND CDM

In this section, we will return to the simplified model introduced in Sec. II, where there are only two components, DE and CDM, in a flat universe. To study this model further, we introduce an interaction between DE and CDM.

In this case, the Friedman equation still reads

$$H^2 = \frac{8\pi G}{3}(\alpha H + \rho_m),$$

and conservation equations are modified to be

$$\dot{\rho}_m + 3H\rho_m = Q, \qquad \dot{\rho}_{\rm DE} + 3(1+\omega)H\rho_{\rm DE} = -Q,$$

where Q denotes the interaction between DE and CDM. Since a generic form of Q is not available, we consider three forms which are often discussed in the literature: $Q = 3\bar{\alpha}H\rho_{\rm DE}$, $3\bar{\beta}H\rho_m$, and $3\bar{\gamma}H\rho_{\rm tot}$, where $\bar{\alpha}$, $\bar{\beta}$, and $\bar{\gamma}$ are three constants, (see e.g. [45] for more references). These forms imply that energy transfers in a Hubble time is proportional to energy density of DE, CDM, and DE + CDM, respectively, and that energy transfers from DE to CDM if $\bar{\alpha}$, $\bar{\beta}$, $\bar{\gamma} > 0$ and vice versa.

In terms of dimensionless quantities, we have

$$1 = \Omega_{\rm DE} + \Omega_m, \tag{13}$$

$$\frac{8\pi G}{3H^2}Q = \dot{\Omega}_m + 2\frac{\dot{H}}{H}\Omega_m + 3H\Omega_m, \tag{14}$$

$$-\frac{8\pi G}{3H^2}Q = \dot{\Omega}_{\rm DE} + 2\frac{\dot{H}}{H}\Omega_{\rm DE} + 3(1+\omega)H\Omega_{\rm DE}, \tag{15}$$

where $\Omega_{\rm DE} = \frac{8\pi G}{3H^2}\rho_{\rm DE}$, $\Omega_m = \frac{8\pi G}{3H^2}\rho_m$ is dimensionless energy density of DE and CDM, respectively. In addition, by use of the linear relation between $\rho_{\rm DE}$ and H, we have

$$H\Omega_{\rm DE} = H_0\Omega_{\rm DE0} = \text{const.} \tag{16}$$

Combining (13) and (14), one can get

$$-\dot{\Omega}_{\rm DE}+2\frac{\dot{H}}{H}(1-\Omega_{\rm DE})+3H(1-\Omega_{\rm DE})=\frac{8\pi G}{3H^2}Q. \tag{17}$$

Putting (15) to eliminate Q, we arrive at

$$2\dot{H}+3\omega H^2\Omega_{\rm DE}+3H^2=0. \tag{18}$$

Then from (17) and (16), one can have the equation of motion of $\Omega_{\rm DE}$ as

$$-\dot{\Omega}_{\rm DE}\frac{2-\Omega_{\rm DE}}{\Omega_{\rm DE}}+3H_0\Omega_{\rm DE0}\frac{1-\Omega_{\rm DE}}{\Omega_{\rm DE}}=\frac{8\pi G}{3H^2}Q \equiv H_0\Omega_{\rm DE0}\Omega_Q, \tag{19}$$

where

$$\Omega_Q=\begin{cases}3\bar{\alpha}, & \text{when } Q=3\bar{\alpha}H\rho_{\rm DE}\\ 3\bar{\beta}\frac{1-\Omega_{\rm DE}}{\Omega_{\rm DE}}, & \text{when } Q=3\bar{\beta}H\rho_m\\ 3\bar{\gamma}\frac{1}{\Omega_{\rm DE}}, & \text{when } Q=3\bar{\gamma}H\rho_{\rm tot}\end{cases}.$$

Expressing this equation in terms of e-folding number $N\equiv\ln a$, and making use of $\frac{d\Omega_{\rm DE}}{dt}=\frac{d\Omega_{\rm DE}}{dN}H_0\Omega_{\rm DE0}/\Omega_{\rm DE}$, we obtain

$$-\Omega'_{\rm DE}\frac{2-\Omega_{\rm DE}}{\Omega^2_{\rm DE}}+3\frac{1-\Omega_{\rm DE}}{\Omega_{\rm DE}}=\Omega_Q. \tag{20}$$

Using (16), (18), and (19), we can get the EoS of the DE

$$\omega=-\frac{1}{2-\Omega_{\rm DE}}-\frac{2}{3}\frac{\Omega_Q}{2-\Omega_{\rm DE}}, \tag{21}$$

while the EoS of the total fluid is

$$\omega_{\rm tot}=-1-\frac{2}{3}\frac{\dot{H}}{H^2}=\omega\Omega_{\rm DE}\ ; \tag{22}$$

in the second equality, we have used (18). In addition, the deceleration parameter is given by

$$q\equiv-\frac{\ddot{a}a}{\dot{a}^2}=\frac{1-2\Omega_{\rm DE}}{2-\Omega_{\rm DE}}-\frac{\Omega_Q\Omega_{\rm DE}}{2-\Omega_{\rm DE}}. \tag{23}$$

We will solve $\Omega_{\rm DE}$, ω, and $\omega_{\rm tot}$ analytically for each Q in the following. However, for the sake of briefness, we will discuss the case of $Q=3\bar{\alpha}H\rho_{\rm DE}$ in some detail only.

A. $Q=3\bar{\alpha}H\rho_{\rm DE}$

In this case, (20) becomes

$$-\Omega'_{\rm DE}(2-\Omega_{\rm DE})+3\Omega_{\rm DE}-3(\bar{\alpha}+1)\Omega^2_{\rm DE}=0.$$

Its solution is

$$3N+C=2\ln\Omega_{\rm DE}-\frac{1+2\bar{\alpha}}{1+\bar{\alpha}}\ln|1-(\bar{\alpha}+1)\Omega_{\rm DE}|, \tag{24}$$

where the integration constant $C=2\ln\Omega_{\rm DE0}-\frac{1+2\bar{\alpha}}{1+\bar{\alpha}}\ln|1-(\bar{\alpha}+1)\Omega_{\rm DE0}|$; $\Omega_{\rm DE0}$ is the dimensionless energy density of DE at present.

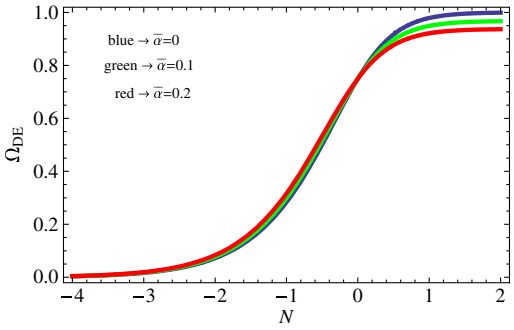

FIG. 7 (color online). $\Omega_{\rm DE}\sim N$, where N is e-folding number. Here $\Omega_{\rm DE0}=0.75$. The blue, green, and red curves correspond to $\bar{\alpha}=0$, 0.1, and 0.2, respectively.

If $\bar{\alpha}<0$, from the solution (24), we can see that $\Omega_{\rm DE}$ can be larger than 1 at late time which is unphysical. This unphysical result comes from the fact that the assumption on energy transfer rate $Q\propto\rho_{\rm DE}$ is oversimplified. For $\bar{\alpha}<0$, DE will gain energy from CDM and energy density of CDM will become less and less. At some time, ρ_m becomes zero, and it is impossible to keep on transferring energy to DE. But due to the oversimplified assumption on Q, CDM will continue to lose energy which is incorrect physically. Therefore, we will presume $\alpha>0$ in this subsection.

From (24) one has $(\bar{\alpha}+1)\Omega_{\rm DE}<1$. It means that for $\bar{\alpha}>0$, $\Omega_{\rm DE}$ will tend to a constant $1/(1+\bar{\alpha})$ rather than 1. The relation of $\Omega_{\rm DE}\sim N$ is shown in Fig. 7; it also indicates that when $\bar{\alpha}$ is larger, the evolution of $\Omega_{\rm DE}$ will be flatter since more energy is injected into CDM. Of course there is an upper limit for $\bar{\alpha}$, as $\Omega_{\rm DE}$ must be able to reach its present value $\Omega_{\rm DE0}\sim0.75$. For $\bar{\alpha}>0$, the coincidence problem can be alleviated excellently, and if $\bar{\alpha}\sim-1+1/\Omega_{\rm DE0}$, this problem is completely solved. The similar situation occurs as $Q\sim\rho_{\rm tot}$ (see Sec. IV C).

In this case, the equation of state of DE is

$$\omega=-\frac{1+2\bar{\alpha}}{2-\Omega_{\rm DE}}.$$

We plot the relation $\omega\sim N$ in Fig. 8. We have shown in Sec. II, it is impossible for ω to cross phantom divide without interaction. Nevertheless from this figure we can see that the situation is changed with the help of interaction term. ω will cross -1 from the quintessence regime to phantom regime and approach to $-1-2\bar{\alpha}$ at late time when $\bar{\alpha}\neq0$.

Finally, the equation of state of the total fluid is

$$\omega_{\rm tot}=-(1+2\bar{\alpha})\frac{\Omega_{\rm DE}}{2-\Omega_{\rm DE}},$$

and it is plotted in Fig. 9. As we expect again, $\omega_{\rm tot}$ can be smaller than -1 in the presence of interaction term and reaches its asymptotic value $-1-2\bar{\alpha}<-1$ at late time. Therefore, in this model the universe will end with the big

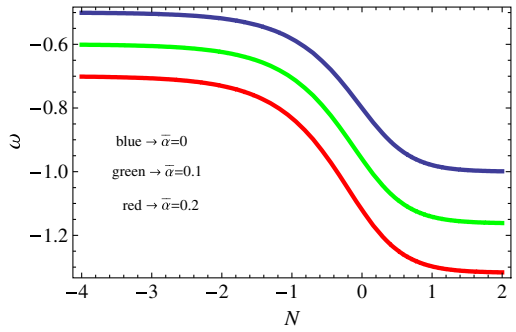

FIG. 8 (color online). $\omega \sim N$, where N is e-folding number. Here $\Omega_{\mathrm{DE0}} = 0.75$. The blue, green, and red curves correspond to $\bar{\alpha} = 0$, 0.1, and 0.2, respectively.

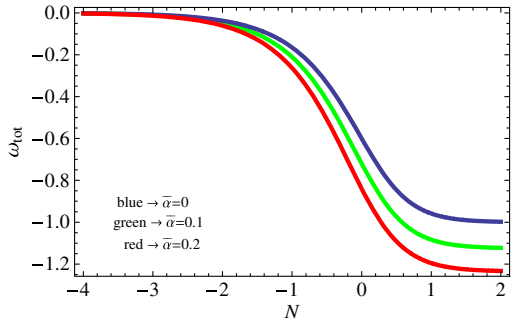

FIG. 9 (color online). $\omega_{\mathrm{tot}} \sim N$, where N is e-folding number. Here $\Omega_{\mathrm{DE0}} = 0.75$. The blue, green, and red curves correspond to $\bar{\alpha} = 0$, 0.1, and 0.2, respectively.

rip singularity in the future [46–48]. And from this figure, we can see that the universe begins to accelerate earlier with larger $\bar{\alpha}$. Note that according to the calculations in Secs. II and III, the universe begins to accelerate at $z_{\mathrm{acc},\bar{\alpha}=0} = 0.6$ in the case without interaction. Thus the acceleration of the universe occurs at $z_{\mathrm{acc},\bar{\alpha}} > 0.6$ when the interaction is present if one keeps $\Omega_{m0} = 0.257$.

B. $Q = 3\bar{\beta}H\rho_m$

In this case, (23) becomes

$$-(2-\Omega_{\mathrm{DE}})\Omega'_{\mathrm{DE}} + 3(1-\bar{\beta})\Omega_{\mathrm{DE}}(1-\Omega_{\mathrm{DE}}) = 0.$$

Its analytical solution reads

$$3(1-\beta)N + C = 2\ln\Omega_{\mathrm{DE}} - \ln(1-\Omega_{\mathrm{DE}}),$$

where the integration constant $C = 2\ln\Omega_{\mathrm{DE0}} - \ln(1-\Omega_{\mathrm{DE0}})$. We can see from the analytical solution that Ω_{DE} varies from 0 at early time to 1 at late time. The EoS of DE is

$$\omega = -\frac{1}{2-\Omega_{\mathrm{DE}}} - 2\bar{\beta}\frac{1}{2-\Omega_{\mathrm{DE}}}\frac{1-\Omega_{\mathrm{DE}}}{\Omega_{\mathrm{DE}}}.$$

One can see in this case that at early time $\omega \to -\bar{\beta}/\Omega_{\mathrm{DE}}$ as $\Omega_{\mathrm{DE}} \to 0$. The plot is shown in Fig. 10. If $\bar{\beta} > 0$, ω will increase from $-\infty$ to some local maximum at some point

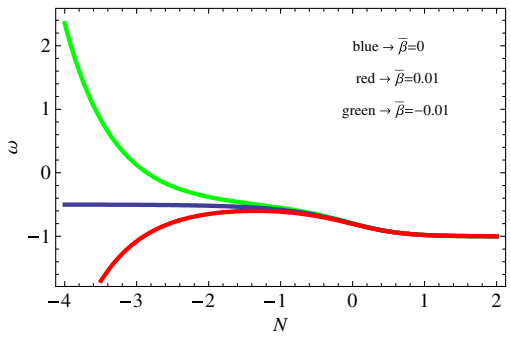

FIG. 10 (color online). $\omega \sim N$ where N is e-folding-number. Here $\Omega_{\mathrm{DE0}} = 0.75$. Blue, green, and red curves correspond to $\bar{\beta} = 0$, -0.01, and 0.01, respectively.

and then decrease to its asymptotic value -1 at late time. Unlike the situation we have discussed in Sec. IVA, ω will cross -1 from phantom regime to quintessence regime in this case. If $\bar{\beta} < 0$, ω will decay monotonically from $+\infty$ to -1 and never cross -1. However, no matter what the value of $\bar{\beta}$ is, the late-time asymptotic behaviors of ω are all the same.

Finally, the EoS of the total fluid is

$$\omega_{\mathrm{tot}} = -\frac{2\bar{\beta} + (1-2\bar{\beta})\Omega_{\mathrm{DE}}}{2-\Omega_{\mathrm{DE}}} = \begin{cases} -\bar{\beta} & \text{at early time} \\ -1 & \text{at late time.} \end{cases}$$

The reasonable value of $\bar{\beta}$ should be $|\bar{\beta}| < 1$. Thus the big rip singularity will be avoided in this case.

C. $Q = 3\bar{\gamma}H\rho_{\mathrm{tot}}$

In this case (20) becomes

$$-\Omega'_{\mathrm{DE}}\frac{2-\Omega_{\mathrm{DE}}}{\Omega_{\mathrm{DE}}^2} + 3\frac{1-\Omega_{\mathrm{DE}}}{\Omega_{\mathrm{DE}}} = 3\bar{\gamma}\frac{1}{\Omega_{\mathrm{DE}}}.$$

Its analytical solution reads

$$3N + C = \frac{2}{1-\bar{\gamma}}\ln\Omega_{\mathrm{DE}} - \left(\frac{1+\bar{\gamma}}{1-\bar{\gamma}}\right)\ln|1-\bar{\gamma}-\Omega_{\mathrm{DE}}|,$$

where $C = \frac{2}{1-\bar{\gamma}}\ln\Omega_{\mathrm{DE0}} - (\frac{1+\bar{\gamma}}{1-\bar{\gamma}})\ln|1-\bar{\gamma}-\Omega_{\mathrm{DE0}}|$. The EoS of DE

$$\omega = -\frac{1}{2-\Omega_{\mathrm{DE}}} - 2\frac{\bar{\gamma}}{2-\Omega_{\mathrm{DE}}}\frac{1}{\Omega_{\mathrm{DE}}}.$$

Once again ω will diverge at early time when the interaction is present. The EoS of the total fluid is

$$\omega_{\mathrm{tot}} = -\frac{2\bar{\gamma}}{2-\Omega_{\mathrm{DE}}} - \frac{\Omega_{\mathrm{DE}}}{2-\Omega_{\mathrm{DE}}}.$$

V. CONCLUSION AND DISCUSSION

In this note we investigated a DE model whose energy density is proportional to Hubble parameter with

a coefficient which is roughly order of $\Lambda^3_{\rm QCD}$. It gives the right order of magnitude of observed energy density of DE. We studied its cosmological evolution. In this DE model, the universe has a de Sitter phase at late time and begins to accelerate at redshift around $z_{\rm acc} \sim 0.6$.

We also fitted this model with observational data including SnIa, BAO, CMB, BBN, and Hubble parameter data. The best-fit values of parameters of the model are $\Omega_{m0} = 0.257$, $h = 0.662$, $\Omega_{b0} = 0.054$. However, the minimal χ^2 gives $\chi^2_{\rm min} = 607.192$, while in the ΛCDM model, $\chi^2_{\Lambda\rm CDM} = 554.264$ for the same data sets. Namely, the simple χ^2 analysis seemingly implies that current data do not favor the ghost DE model, compared to the ΛCDM model. Clearly this result is not conclusive, further study is needed. For example, we further studied the cosmological dynamics of the model by considering there exists some interaction between DE and CDM. Three kinds of interaction forms are discussed. The interaction will modify the dynamics of the model.

We found that the squared adiabatic sound speed of the DE is negative. However, one cannot conclude this model is unstable since the stability is determined by dynamical sound speed rather than the adiabatic sound speed. In addition, the negative squared adiabatic sound speed should not be treated as a signal for instability of the theory since the Veneziano ghost is not a propagating physical degree of freedom. The stability of this model should be studied seriously by investigating linearized Einstein equations, which are currently under investigation. If there exists instability, the ghost DE model has to be further modified or to be abandoned.

ACKNOWLEDGMENTS

We thank A. Christopherson for helpful correspondence and the referee for suggestive comments. R. G. C. thanks N. Ohta for various valuable discussions on the QCD ghost. H. B. Z. thanks Bin Hu for helpful discussions. This work was supported in part by the National Natural Science Foundation of China (Grants No. 10821504, No. 10975168, and No. 11035008), and by the Ministry of Science and Technology of China under Grant No. 2010CB833004, and also by a grant from the Chinese Academy of Sciences.

[1] A. G. Riess *et al.* (Supernova Search Team Collaboration), Astron. J. **116**, 1009 (1998); S. Perlmutter *et al.* (Supernova Cosmology Project Collaboration), Astrophys. J. **517**, 565 (1999).
[2] S. Weinberg, Rev. Mod. Phys. **61**, 1 (1989); arXiv: astro-ph/0005265; V. Sahni and A. A. Starobinsky, Int. J. Mod. Phys. D **9**, 373 (2000); S. M. Carroll, Living Rev. Relativity **4**, 1 (2001); P. J. E. Peebles and B. Ratra, Rev. Mod. Phys. **75**, 559 (2003); T. Padmanabhan, Phys. Rep. **380**, 235 (2003); E. J. Copeland, M. Sami, and S. Tsujikawa, Int. J. Mod. Phys. D **15**, 1753 (2006).
[3] E. J. Copeland, M. Sami, and S. Tsujikawa, Int. J. Mod. Phys. D **15**, 1753 (2006).
[4] R. R. Caldwell and P. J. Steinhardt, Phys. Rev. D **57**, 6057 (1998).
[5] P. J. Steinhardt, L. M. Wang, and I. Zlatev, Phys. Rev. D **59**, 123504 (1999).
[6] S. Capozziello, S. Carloni, and A. Troisi, Recent Res. Dev. Astron. Astrophys. **1**, 625 (2003).
[7] M. Li, Phys. Lett. B **603**, 1 (2004); R. G. Cai, Phys. Lett. B **657**, 228 (2007); H. Wei and R. G. Cai, Phys. Lett. B **660**, 113 (2008); M. X. Luo and Q. P. Su, Phys. Lett. B **626**, 7 (2005); B. Feng, X. L. Wang, and X. M. Zhang, Phys. Lett. B **607**, 35 (2005); C. Gao, X. Chen, and Y. G. Shen, Phys. Rev. D **79**, 043511 (2009).
[8] S. Nojiri and S. D. Odintsov, Phys. Rev. D **72**, 023003 (2005); S. Capozziello, V. F. Cardone, E. Elizalde, S. Nojiri, and S. D. Odintsov, Phys. Rev. D **73**, 043512 (2006).
[9] S. Nojiri and S. D. Odintsov, Phys. Rev. D **68**, 123512 (2003); Phys. Rep. **505**, 59 (2011).
[10] F. R. Urban and A. R. Zhitnitsky, Phys. Lett. B **688**, 9 (2010); Phys. Rev. D **80**, 063001 (2009); J. Cosmol. Astropart. Phys. 09 (2009) 018; Nucl. Phys. B **835**, 135 (2010).
[11] N. Ohta, Phys. Lett. B**695**, 41 (2011).
[12] E. Witten, Nucl. Phys. B **156**, 269 (1979).
[13] G. Veneziano, Nucl. Phys. B **159**, 213 (1979).
[14] C. Rosenzweig, J. Schechter, and C. G. Trahern, Phys. Rev. D **21**, 3388 (1980).
[15] P. Nath and R. L. Arnowitt, Phys. Rev. D **23**, 473 (1981).
[16] K. Kawarabayashi and N. Ohta, Nucl. Phys. B **175**, 477 (1980); Prog. Theor. Phys. **66**, 1789 (1981); N. Ohta, Prog. Theor. Phys. **66**, 1408 (1981).
[17] A. R. Zhitnitsky, Phys. Rev. D **82**, 103520 (2010).
[18] B. Holdom, Phys. Lett. B **697**, 351 (2011).
[19] A. R. Zhitnitsky, arXiv:1105.6088.
[20] E. Thomas and A. R. Zhitnitsky, arXiv:1109.2608.
[21] J. Bjorken, arXiv:hep-th/0111196.
[22] R. Schutzhold, Phys. Rev. Lett. **89**, 081302 (2002).
[23] J. D. Bjorken, arXiv:astro-ph/0404233.
[24] F. R. Klinkhamer and G. E. Volovik, Phys. Rev. D **77**, 085015 (2008).
[25] F. R. Klinkhamer and G. E. Volovik, Phys. Rev. D **78**, 063528 (2008).
[26] F. R. Klinkhamer and G. E. Volovik, Phys. Rev. D **79**, 063527 (2009).
[27] Y. B. Zeldovich, Pis'ma Zh. Eksp. Teor. Fiz. **6**, 883 (1967) [JETP Lett. **6**, 316 (1967)].

[28] R. Amanullah *et al.*, Astrophys. J. **716**, 712 (2010).
[29] W. J. Percival *et al.*, Mon. Not. R. Astron. Soc. **401**, 2148 (2010).
[30] E. Komatsu *et al.*, Astrophys. J. Suppl. Ser. **192**, 18 (2011).
[31] J. Simon, L. Verde, and R. Jimenez, Phys. Rev. D **71**, 123001 (2005).
[32] E. Gaztanaga, A. Cabre, and L. Hui, Mon. Not. R. Astron. Soc. **399**, 1663 (2009).
[33] P. Serra, A. Cooray, D. E. Holz, A. Melchiorri, S. Pandolfi, and D. Sarkar, Phys. Rev. D **80**, 121302 (2009).
[34] S. Burles, K. M. Nollett, and M. S. Turner, Astrophys. J. **552**, L1 (2001).
[35] G. R. Dvali, G. Gabadadze, and M. Porrati, Phys. Lett. B **485**, 208 (2000); C. Deffayet, Phys. Lett. B **502**, 199 (2001).
[36] R. Maartens and K. Koyama, Living Rev. Relativity **13**, 5 (2010).
[37] R. R. Caldwell and E. V. Linder, Phys. Rev. Lett. **95**, 141301 (2005).
[38] A. J. Christopherson and K. A. Malik, Phys. Lett. B **675**, 159 (2009).
[39] C. Deffayet, O. Pujolas, I. Sawicki, and A. Vikman, J. Cosmol. Astropart. Phys. 10 (2010) 026.
[40] S. Nesseris and L. Perivolaropoulos, Phys. Rev. D **72**, 123519 (2005).
[41] D. J. Eisenstein and W. Hu, Astrophys. J. **496**, 605 (1998).
[42] W. Hu and N. Sugiyama, Astrophys. J. **471**, 542 (1996).
[43] S. Basilakos, M. Plionis, and J. Sola, Phys. Rev. D **80**, 083511 (2009).
[44] M. Chevallier and D. Polarski, Int. J. Mod. Phys. D **10**, 213 (2001); E. V. Linder, Phys. Rev. Lett. **90**, 091301 (2003); D. Huterer and G. Starkman, Phys. Rev. Lett. **90**, 031301 (2003); D. Huterer and A. Cooray, Phys. Rev. D **71**, 023506 (2005); A. Hojjati, L. Pogosian, and G. B. Zhao, arXiv:0912.4843.Y. Wang, Phys. Rev. D **80**, 123525 (2009); S. Sullivan, A. Cooray, and D. E. Holz, J. Cosmol. Astropart. Phys. 09 (2007) 004; G. B. Zhao, D. Huterer, and X. Zhang, Phys. Rev. D **77**, 121302 (2008); P. Serra, A. Cooray, D. E. Holz, A. Melchiorri, S. Pandolfi, and D. Sarkar, Phys. Rev. D **80**, 121302 (2009); Y. Gong, R. G. Cai, Y. Chen, and Z. H. Zhu, arXiv:0909.0596; R. G. Cai, Q. Su, and H. B. Zhang, J. Cosmol. Astropart. Phys. 04 (2010) 012.
[45] H. Wei and R. G. Cai, Eur. Phys. J. C **59**, 99 (2008); R. G. Cai and Q. Su, Phys. Rev. D **81**, 103514 (2010).
[46] R. R. Caldwell, M. Kamionkowski, and N. N. Weinberg, Phys. Rev. Lett. **91**, 071301 (2003).
[47] S. M. Carroll, M. Hoffman, and M. Trodden, Phys. Rev. D **68**, 023509 (2003).
[48] J. M. Cline, S. Y. Jeon, and G. D. Moore, Phys. Rev. D **70**, 043543 (2004).